Strong field atomic ionization dynamics: role of the Coulomb potential studied by means of a model.

S. Giraud[a], B. Piraux[b], Yu.V. Popov[c] and H.M. Tetchou Nganso[b]

[a] Ecole Normale Supérieure de Cachan, Antenne de Bretagne,
Avenue Robert Schuman, Campus de Ker Lann, F-35170 Bruz, France
[b] Laboratoire de Physique Atomique, Moléculaire et Optique (PAMO),
Université catholique de Louvain, 2, chemin du Cyclotron,
B-1348 Louvain-la-Neuve, Belgium*
[c] Nuclear Physics Institute, Moscow State University, Moscow, 119992, Russia†

ABSTRACT

We consider the multiphoton ionization of a one-active electron system exposed to an intense low-frequency laser pulse. We describe a model that is aimed at studying the role of the Coulomb potential in a regime where tunneling ionization is assumed to be the dominant ionization mechanism. In particular, we hope to explain why the low energy part of the above-threshold ionization spectrum is not well reproduced by the Keldysh-type theories.

Keywords: multiphoton ionization, tunnel ionization,time-dependent Schrödinger equation

1. INTRODUCTION

In his pioneering work on the ionization dynamics of atoms exposed to strong, long wavelength electromagnetic fields, Keldysh[1] introduced the so-called adiabaticity parameter $\gamma = \frac{\omega}{E}\sqrt{2I_p}$ where I_p is the ionization potential, ω the field frequency, and E its amplitude. This parameter allows to distinguish two ionization mechanisms: for $\gamma \ll 1$ (low frequency, high intensity), the electric field is quasi-static and ionization occurs through tunnelling while for $\gamma \gg 1$, multiphoton ionization prevails.

Keldysh theory leads to an ionization rate as a function of intensity and frequency which is in fair (at least qualitatively) agreement with the experimental data. However, Keldysh himself was aware of serious problems inherent to his theory as for instance the fact that his expression for the ionization probability contains the correct exponential factor but the wrong coefficient in the static limit $\omega \to 0$. He connected this problem with the approximation made on the final state of the ejected electron. In addition, his approach does not apply, strictly speaking, to the ionization of atoms but rather, to the ionization of negative ions since the escaping electron is described as a Volkov state.

Keldysh approach has been generalized to the treatment of the ionization of atoms.[2] In parallel, various numerical methods aimed at solving the time-dependent Schrödinger equation (TDSE) in the case of atomic hydrogen have been developped.[3–6] The results clearly show that Keldysh approahes satisfactorily account for many features of the electron energy spectra, in particular at high energy. However, the low energy part of the electron energy spectrum (below twice the ponderomotive potential) is not well reproduced by Keldysh approaches. Note that it is precisely this part of the spectrum that dominates the total ionization rate. The origin of this discrepancy is directly related to the way the Coulomb potential is treated. It is legitimate to neglect the influence of the Coulomb potential compared to the external field once the electron has tunnelled out. However, the numerical solution of the TDSE has shown[6] that even when tunnelling is expected to dominate, many electrons reach the continuum while staying close to the nucleus where the Coulomb potential dominates. This point has been confirmed by a recent results of the experimental team of Ullrich[7] where a clear signature of the Coulomb potential namely a resonant structure in the above-threshold ionization spectrum has been observed.

* e-mail: piraux@pamo.ucl.ac.be
† e-mail: popov@srd.sinp.msu.ru

Purely numerical schemes are usually not transparent enough giving little insight of the ionization dynamics. In this context, the actual role of the Coulomb potential is far to be understood. The main objective of our work is to try to understand this role and to define under what conditions it is significant. In this contribution, we present a 3D model. It is based on the TDSE in momentum space; the Coulomb potential is replaced by a non-local separable potential. This latter one is built in such a way that it supports only one bound state having the same energy as the ground state of atomic hydrogen. In the configuration space, the ground state electron experiences the exact Coulomb potential while the other electrons "feel" a short range potential. Within this approximation, the solution of the TDSE reduces to the solution of a 1D Volterra integral equation of the second kind for a function $F(t)$ that contains all the dynamics. An extremely fast and accurate numerical code has been developed to solve this equation. The next step consists in introducing components in the expression of the separable potential in order to take into account exactly various bound states of atomic hydrogen.

We actually consider a symmetric attractive separable potential (the atomic units $\hbar = e = m_e = 1$ are used throughout):

$$V(\vec{p}, \vec{p}\,') = -\sum_{n=1}^{N} v_n(\vec{p}) v_n^*(\vec{p}\,'), \tag{1}$$

which we are going to use as a separable analogue of the Coulomb potential $V(r) = -Z/r$ in momentum-space. We demand from this potential to reproduce N eigenfunctions and eigenenergies of the Coulomb spectrum. The momentum space representation of the bound state ϕ_j satisfies the following equation:

$$(\varepsilon_j - \frac{1}{2}p^2)\varphi_j(\vec{p}) + \sum_{n=1}^{N} a_{jn} v_n(\vec{p}) = 0, \tag{2}$$

where

$$a_{jn} = \int \frac{d^3p'}{(2\pi)^3} v_n^*(\vec{p}\,')\varphi_j(\vec{p}\,'). \tag{3}$$

Eq. (2) may be written in matrix form as follows:

$$\mathbf{\Phi} = -\mathbf{A}\mathbf{V}, \tag{4}$$

where $\mathbf{A}$ is a symmetric $N \times N$ matrix of elements a_{jn}. $\mathbf{\Phi}$ and $\mathbf{V}$ are $N \times 1$ vectors whose elements are the $v_n(\vec{p})$ and $(\varepsilon_j - \frac{1}{2}p^2)\varphi_j(\vec{p})$ respectively. Consequently,

$$\mathbf{V} = -\mathbf{A}^{-1}\mathbf{\Phi}. \tag{5}$$

On the other hand, from Eq. (3) we have:

$$\mathbf{A} = (\mathbf{A}^{\mathbf{T}})^{-1}\ \mathbf{\Gamma},\ \text{or}\ \mathbf{A}\mathbf{A}^{\mathbf{T}} = \mathbf{\Gamma}, \tag{6}$$

where $\mathbf{A}^{\mathbf{T}}$ denotes the transpose matrix $\mathbf{A}$. The elements of the symmetric $N \times N$ matrix $\mathbf{\Gamma}$ are given by:

$$\gamma_{ij} = -\int \frac{d^3p}{(2\pi)^3}\varphi_i^*(\vec{p})(\varepsilon_j - \frac{1}{2}p^2)\varphi_j(\vec{p}) = Z\int \frac{d^3r}{r}\tilde{\varphi}_i^*(\vec{r})\tilde{\varphi}_j(\vec{r}), \tag{7}$$

where $\tilde{\varphi}_j(\vec{r})$ is the wavefunction associated to a Coulomb bound state in the configuration space.

The present approach is a general scheme for the factorization of the Coulomb potential. It consists in replacing the Coulomb potential in momentum space by a sum of non-local separable potentials built in such a way that they keep the correct characteristics of the exact Coulomb potential for the bound electrons. It is therefore providing a way of analyzing how the atomic structure associated to the Coulomb potential influences the ionization dynamics. In the present contribution which is a progress report, we limit ourselves to only one term in the expansion of the non-local Coulomb potential, namely the term associated to the ground state.

2. THEORY

The TDSE in momentum space for atomic hydrogen exposed to a laser field linearly polarized along the unit vector $\vec{e}$ writes:

$$\left[i\frac{\partial}{\partial t} - \frac{p^2}{2} - \frac{1}{c}A(t)(\vec{e}\,\vec{p})\right]\Phi(\vec{p},t) - \int \frac{d^3p\,'}{(2\pi)^3}V(\vec{p},\vec{p}\,')\Phi(\vec{p}\,',t) = 0; \quad \Phi(\vec{p},0) = \frac{8\sqrt{\pi}}{(p^2+1)^2}. \tag{8}$$

where the kernel $V(\vec{p},\vec{p}\,')$ is given by:

$$V(\vec{p},\vec{p}\,') = -\frac{4\pi}{|\vec{p}-\vec{p}\,'|^2}. \tag{9}$$

We normalize the wavepacket in the following way:

$$\int \frac{d^3p}{(2\pi)^3}|\Phi(\vec{p},t)|^2 = 1. \tag{10}$$

We assume the laser pulse with a sine square envelope and define the potential vector as follows:

$$A(t) = A_0\sin^2(\pi\frac{t}{T})\sin(\omega t)\ (0 \le t \le T); \quad A(t) = 0\ (t \le T); \quad \frac{A_0}{c} = \frac{1}{\omega}\sqrt{\frac{I}{I_0}}. \tag{11}$$

In Eqs. (11), I is the peak intensity of the laser pulse and $I_0 = 3.5\times10^{16}\ W/cm^2$, the atomic unit of intensity. ω is the laser frequency and $T = 2\pi n/\omega$, the total pulse duration with n indicating the total number of optical cycles.

We now perform the following substitution for the Coulomb kernel in Eq. (8):

$$V(\vec{p},\vec{p}\,') \to -\frac{16\pi}{(p^2+1)(p'^2+1)}. \tag{12}$$

We then obtain the equation:

$$\left[i\frac{\partial}{\partial t} - \frac{p^2}{2} - \frac{1}{c}A(t)(\vec{e}\vec{p})\right]\Phi(\vec{p},t) + F(t)\frac{16\pi}{(p^2+1)} = 0; \quad F(t) = \int \frac{d^3p\,'}{(2\pi)^3}\frac{\Phi(\vec{p}\,',t)}{(p'^2+1)}. \tag{13}$$

Its solution takes the form:

$$\Phi(\vec{p},t) = \exp\left(-i\frac{p^2}{2}t + ib(t)(\vec{e}\vec{p})\right)\left[\Phi(\vec{p},0) + \frac{16i\pi}{(p^2+1)}\int_0^t F(\xi)\exp\left(i\frac{p^2}{2}\xi - ib(\xi)(\vec{e}\vec{p})\right)d\xi\right], \tag{14}$$

with $b(t) = -\frac{1}{c}\int_0^t A(\xi)d\xi$. By inserting (14) into (13), we get the Volterra integral equation for the function $F(t)$:

$$F(t) = F_0(t) + \int_0^t K(t,s)F(s)ds, \tag{15}$$

where

$$F_0(t) = \int \frac{d^3p}{(2\pi)^3}\frac{\Phi(\vec{p},0)}{(p^2+1)}\exp\left(-i\frac{p^2}{2}t + ib(t)(\vec{e}\vec{p})\right), \tag{16}$$

and

$$K(t,s) = 16i\pi\int \frac{d^3p}{(2\pi)^3}\frac{1}{(p^2+1)^2}\exp\left(-i\frac{p^2}{2}(t-s) + i(b(t)-b(s))(\vec{e}\vec{p})\right). \tag{17}$$

All integrals present in the above equations can be calculated analytically with the basic formula:

$$I(x,y,\gamma)=\int\limits_{-\infty}^{+\infty}\frac{pdp}{p^2+\gamma}e^{-ixp^2+iyp}=$$

$$\frac{i\pi}{2}e^{ix\gamma}\left\{e^{-y\sqrt{\gamma}}\mathrm{erfc}\left(e^{i\pi/4}\sqrt{\gamma x}-e^{-i\pi/4}\frac{y}{2\sqrt{x}}\right)-e^{y\sqrt{\gamma}}\mathrm{erfc}\left(e^{i\pi/4}\sqrt{\gamma x}+e^{-i\pi/4}\frac{y}{2\sqrt{x}}\right)\right\}. \tag{18}$$

Here,

$$\mathrm{erfc}(z)=1-\frac{2z}{\sqrt{\pi}}\int\limits_0^1 e^{-z^2t^2}dt,$$

is one of the definitions of the complementary error function. Let us define

$$\mathcal{I}_n(x,y)=\frac{1}{2iy}\frac{(-1)^{n-1}}{(n-1)!}\frac{\partial^{n-1}}{\partial\gamma^{n-1}}I(x,y,\gamma)\mid_{\gamma=1}.$$

Accordingly,

$$F_0(t)=\frac{4}{\pi^{3/2}}\mathcal{I}_3\left(\frac{t}{2},b(t)\right),\quad K(t,s)=\frac{8i}{\pi}\mathcal{I}_2\left(\frac{t-s}{2},b(t)-b(s)\right)\quad .$$

In order to calculate the transition amplitudes we have also to calculate the continuum wave-functions. For separable potentials, it is easy to show that:

$$\varphi^{\pm}(\vec{k},\vec{p})=(2\pi)^3\delta(\vec{p}-\vec{k})-\frac{32\pi C^{\pm}(k)}{(p^2+1)((k\pm i\varepsilon)^2-p^2)};\quad C^{\pm}(k)=\frac{1}{k^2+5-8/(1\mp ik)}. \tag{19}$$

The quantity $(\pm i\varepsilon)$ accounts correctly for the singularity. In our calculations, we chose the prescription $(+i\varepsilon)$ corresponding to a set of outgoing waves.

By projecting the wavepacket on the ground state $\varphi_0(\vec{p})\equiv\Phi(\vec{p},0)$, we obtain the amplitude $c_0(t)$ and the probability $|c_0(t)|^2$ for our "hydrogen atom" to stay in the ground state:

$$c_0(t)=<\varphi_0|\Phi(t)>=\frac{32}{\pi}\mathcal{I}_4\left(\frac{t}{2},b(t)\right)+\frac{64i}{\sqrt{\pi}}\int\limits_0^t\mathcal{I}_3\left(\frac{t-s}{2},b(t)-b(s)\right)F(s)ds. \tag{20}$$

Now we introduce the function

$$\mathcal{D}_n(x,y,k)=\frac{1}{y}\int\limits_{-\infty}^{+\infty}\frac{p\ dp}{(p^2+1)^n(p^2-(k-i\varepsilon)^2)}e^{-ixp^2+iyp}=$$

$$\frac{1}{y}\frac{(-1)^n}{(n-1)!}\frac{\partial^{n-1}}{\partial\gamma^{n-1}}\left\{\frac{1}{\gamma+k^2}[I(x,y,\gamma)-I(x,y,-(k-i\varepsilon)^2)]\right\}_{\gamma=1},\quad\sqrt{-(k-i\varepsilon)^2}=ik. \tag{21}$$

The ionization amplitude $c(\vec{k},t)=<\varphi^+(\vec{k})|\Phi(t)>$ can be written in terms of this function as follows:

$$c(\vec{k},t)=\frac{8\sqrt{\pi}}{(k^2+1)^2}\exp\left(-i\frac{k^2}{2}t+ib(t)(\vec{e}\vec{k})\right)+\frac{16i\pi}{(k^2+1)}\int\limits_0^t F(\xi)\exp\left(-i\frac{k^2}{2}(t-\xi)+i(b(t)-b(\xi))(\vec{e}\vec{p})\right)d\xi$$

$$-\frac{64i}{\sqrt{\pi}}C^-(k)\mathcal{D}_3\left(\frac{t}{2},b(t),k\right)+128C^-(k)\int_0^t F(\xi)\ \mathcal{D}_2\left(\frac{t-\xi}{2},b(t)-b(\xi),k\right)d\xi. \tag{22}$$

Finally, the differential probability for an electron to have the energy E can be determined in terms of the spectral density $D(E,t)$:

$$dP=D(E,t)dE,\quad D(E,t)=\frac{\sqrt{2E}}{(2\pi)^3}\int|c(\vec{k},t)|^2d\Omega_k.$$

Obviously,

$$P(t)=1-|c_0(t)|^2=\int_0^{+\infty}D(E,t)dE. \tag{23}$$

An accurate numerical algorithm has been implemented to solve Eq. (15). We use the corresponding computer code to calculate the transition amplitudes (20) and (22).

3. RESULTS AND DISCUSSION

Our model actually reproduces all well known features of the above-threshold ionization spectra as well as the ionization probability. There are however some interesting and unexpected observations requiring a deeper analysis. We discuss these features below. In all our results, the frequency is fixed at 0.057 a.u. (Ti-Saphir laser) and the duration of the pulse is 8 optical cycles. In Fig. 1, we show for various peak intensities, the probability density $|\Phi(p_n=0,p_z,t)|^2$ in logarithmic scale as a function of both the time (in optical cycles) and the projection of the canonical momentum along the polarization axis. Together with these graphs, we also show the ionization probability (the yield) as a function of time.

Although none of these two quantities are observable (during the interaction, they depend on the gauge), they provide however valuable information about the ionization dynamics.[6] For the lowest peak intensity, $I=1\times10^{14}\ W/cm^2$, the atomic system does not ionize. The probability density exhibits oscillations at the laser frequency. On the same graph, we also show the vector potential $A(t)$ (dashed line); we clearly see that the oscillations of the probability density are in phase opposition with those of $A(t)$. In fact, at time $t=0$, the total wavefunction coincides with the 1s-state wavefunction (the only state included). Therefore, these oscillations correspond to the displacement of this state in the momentum space. On the other hand, we know that for the 1s-state, the average velocity (along the polarization axis) $<v_z>\approx 0$ and that in the velocity gauge, the canonical moment is such that

$$\vec{v}=\vec{p}+A(t)\vec{e}. \tag{24}$$

As a result, we found for the 1s-state:

$$<p_z>\approx -A(t). \tag{25}$$

As soon as the peak intensity increases, we start to see vertical stripes that appear after 2 optical cycle. These stripes can be associated to electrons of a given energy in the continuum and therefore to the ionization. Indeed, applying Ehrenfest's theorem to continuum states yields:

$$\frac{d}{dt}<\vec{p}>=-<\vec{\nabla}V>\approx 0. \tag{26}$$

We verified that the energy associated to each stripe $p^2/2$ corresponds exactly to the kinetic energy of the ejected electron. We want to stress here that in contrast to the configuration space, the probability density stays localized in momentum space. The appearance of the stripes can therefore be interpreted as the instantaneous manifestation of the ionization. When the peak intensity increases further, the system ionizes quickly and the

number of stripes corresponding to higher values of the canonical momentum increases significantly. However, we do not observe clear stripes for the small values of p_z. This contrasts sharply with what we observe in the case of the exact Coulomb potential.[6] This raises the question of the role of the other atomic hydrogen bound states in the mechanism of ejection of low energy electrons. This question stays unsolved and calls for the generalization of the present calculation to the case where more than one component are included in the expansion of the Coulomb potential kernel. In Fig. 2, we show the density $|\Phi_{ion}(p_n = 0, p_z; T)|^2 = |\Phi(\vec{p}, T) - c_0(T)\varphi_0(\vec{p})|^2$ in logarithmic scale, as a function of the canonical momentum along the polarization axis p_z at the end of the interaction and for the same cases as in Fig. 1. The vertical dashed line indicate in each case, the value of the canonical momentum corresponding to $2U_p$ and $10U_p$ where $U_p = I/(4\omega^2 I_0) = 1/(4\gamma^2)$ is the ponderomotive potential. Above $2U_p$, the results are in qualitative agreement with those corresponding to the exact Coulomb potential. Below $2U_p$ however, the results obtained with our model strongly underestimate what is expected with the exact Coulomb potential confirming our conclusions about the first graph. The asymmetry that is observed at high peak intensity is due to the fact that the time it takes to the system to ionize is very short.

4. CONCLUSIONS

In this contribution, we presented a model aimed at exploring the role of the coulomb potential in the ejection of low energy electrons from an atom exposed to a strong low frequency pulsed laser field. Although we are in a frequency and intensity regime where tunneling is expected to dominate, our first results already indicate that the atomic structure associated to the Coulomb potential plays a significant role. This question however has to be analyzed more in depth. It calls for a generalization of the present calculations to the case where more than one atomic states are treated exactly within the present model. Furthermore, the present approach clearly show that the momentum space is more natural than the configuration space to study the ionization dynamics.

REFERENCES

1. Keldysh L.V., Sov. Phys. JETP **20** (1965), 1307.
2. Faisal F.H.M., J. Phys. B **6** (1973), L89; Reiss H.R., Phys. Rev. A **22** (1980), 1786; Lewenstein M. *et al.*, Phys. Rev. A **49** (1994), 2117; Lewenstein M. *et al.*, Phys. Rev. A **51** (1995), 1495.
3. Kulander K.C., Schafer K.J., and Krause K.J., Phys. Rev. Lett. **66** (1991), 2601.
4. Huens E. *et al.*, Phys. Rev. A **55** (1997), 2132.
5. Potvliege R.M. and Shakeshaft R., Phys. Rev. A **38** (1988), 1098; ibid. **40** (1989), 3061;
6. de Bohan A., "Thése de Doctorat", Université catholique de Louvain, 2001; de Bohan A. *et al.*, Phys. Rev. Lett. **89** (2002), 113002.
7. Rudenko A. *et al.*, in "Electron and Photon Impact Ionization and Related Topics", IOP Conf. Ser. **183** (2004), 93.

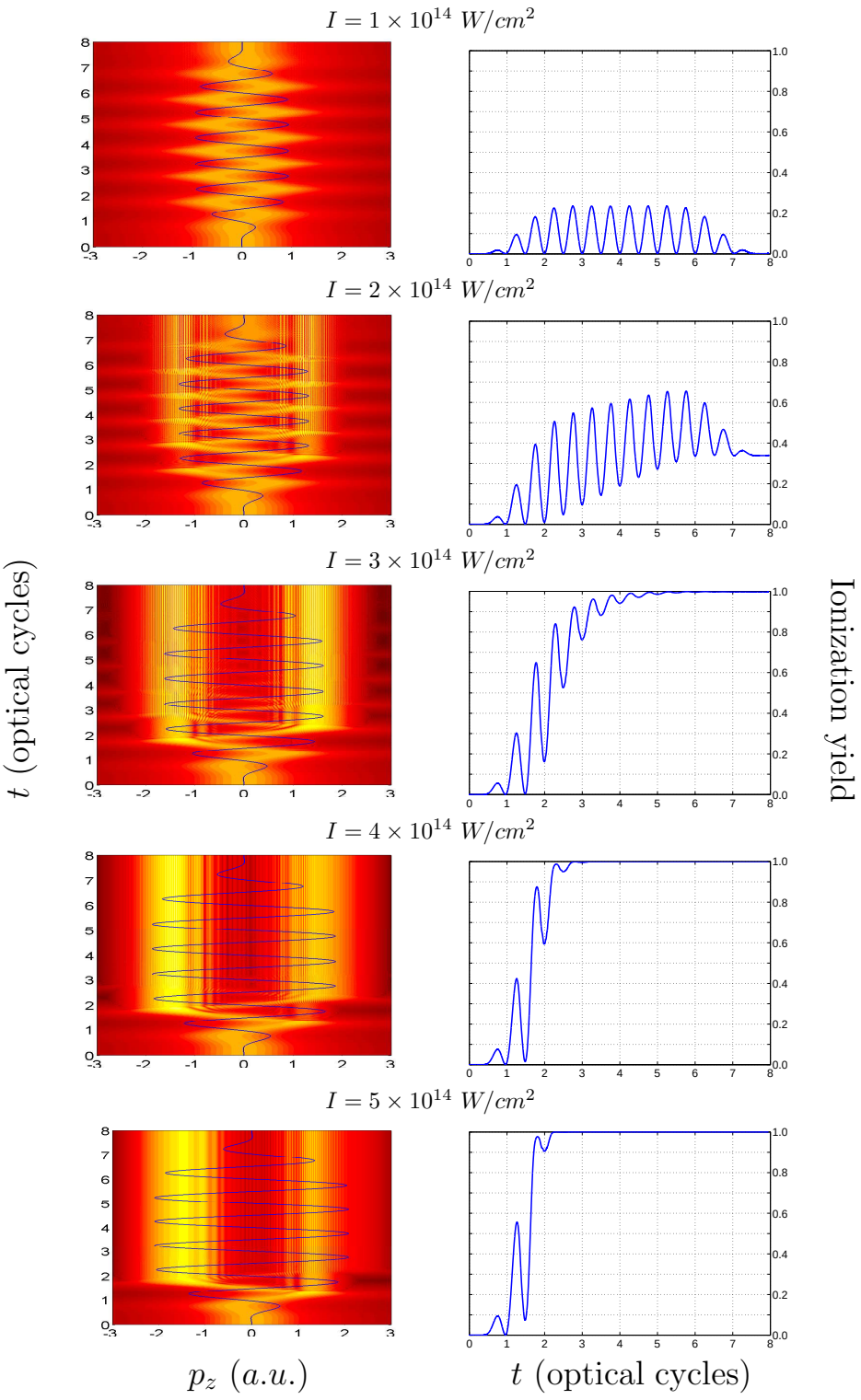

Figure 1. Probability density $|\Phi(p_n = 0, p_z; t)|^2$ (left panel) and the ionization yield $P(t)$ (right panel). The pulse intensity varies between $I = 1 \times 10^{14}$ W/cm^2 and $I = 5 \times 10^{14}$ W/cm^2, $\omega = 0.057$ a.u..The thin oscillating dashed line in the left panels represents the time evolution of the vector potential.

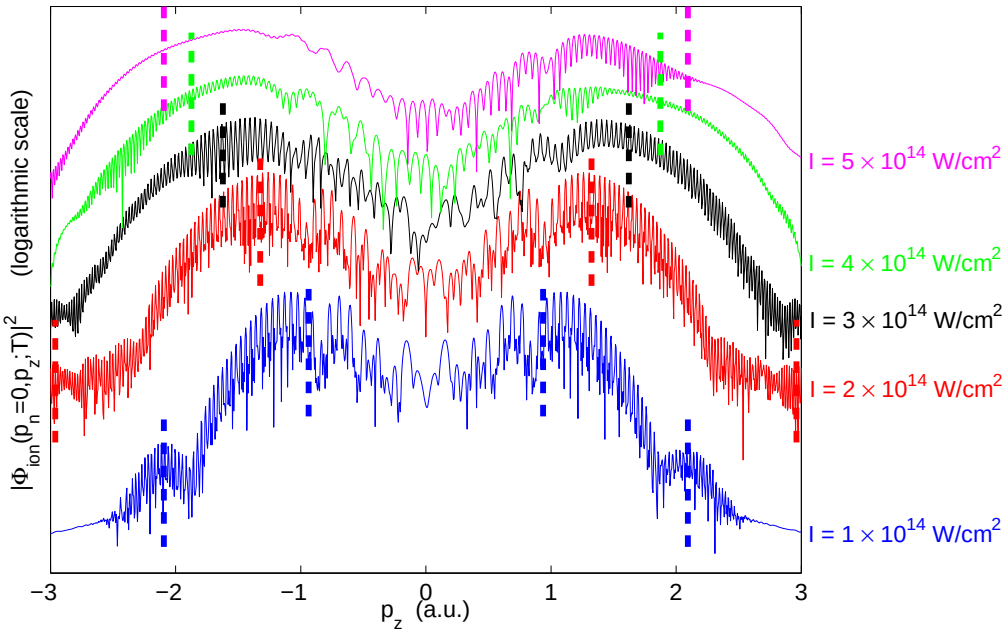

Figure 2. Ionization probability density $|\Phi_{ion}(p_n = 0, p_z; T)|^2$ at the end of the pulse for different intensities, and $\omega = 0.057$ a.u.. The vertical dashed lines indicate the value of p_z corresponding to $2U_p$ and $10U_p$.